

# Cosmic Microwave Background

Student Seminar

**Jildou Baarsma**

0438154

January 2008

Institute for Theoretical Physics,  
Utrecht University

Supervisors  
T. Prokopec  
J.F. Koksma



# Contents

<b>1</b>	<b>History of the Cosmic Microwave Background</b>	<b>5</b>
<b>2</b>	<b>Introduction</b>	<b>7</b>
<b>3</b>	<b>Black Body Spectrum</b>	<b>11</b>
<b>4</b>	<b>Measurements of the CMB</b>	<b>15</b>
4.1	Foreground Subtraction . . . . .	15
4.2	Temperature Fluctuations . . . . .	16
4.3	Future Measurements . . . . .	17
<b>5</b>	<b>Anisotropies in the Cosmic Microwave Background</b>	<b>19</b>
5.1	The Dipole Anisotropy . . . . .	19
5.2	Primary Fluctuations in the CMB . . . . .	21
5.2.1	The ISW rise, $\ell \lesssim 10$ , and Sachs-Wolfe plateau, $10 \lesssim \ell \lesssim 100$ . . . . .	24
5.2.2	The acoustic peaks, $100 \lesssim \ell \lesssim 1000$ . . . . .	26
5.2.3	The damping tail, $\ell \gtrsim 1000$ . . . . .	26
<b>6</b>	<b>Constraints on Theories and Cosmological Parameters</b>	<b>27</b>
<b>7</b>	<b>Polarization</b>	<b>31</b>
	<b>Bibliography</b>	<b>32</b>



# Chapter 1

## History of the Cosmic Microwave Background

The cosmic microwave background radiation was predicted in 1948 by George Gamow and Ralph Alpher. Moreover, they were able to estimate the temperature of this radiation to be 5 K. Two years later they re-estimated this temperature to be 28 K. These results were not widely discussed. Only in the early 1960's they were rediscovered by Yakov Zel'dovich. At the same time Robert Dicke predicted independently these same results.

In 1964 David Todd Wilkinson and Peter Roll, two colleagues of Dicke at Princeton University, began constructing a Dicke radiometer to measure the cosmic background radiation. In 1965 Arno Penzias and Robert Woodrow Wilson also started constructing a Dicke radiometer, not far from Wilkinson and Roll, at Crawford Hill location of Bell Telephone Laboratories in New Jersey. They wanted to use it for radio astronomy and satellite communication experiments. Their radiometer had an excess 3.5 K antenna temperature which they could not account for. This noise was far less energetic than the radiation coming from the Milky Way and moreover, it was isotropic. They assumed their instrument was subject to interference by terrestrial sources. First they thought that their noise was coming from New York City. But this hypothesis was rejected not long thereafter. Then they examined their antenna and saw that it was full of pigeon droppings and thought the noise might come from the pigeons. But after cleaning the antenna and killing all the pigeons, the noise remained. After rejecting all possible sources for noise, Penzias and Wilson published their findings. The signal they were receiving was identified with the cosmic microwave background shortly after their publication. Penzias and Wilson received the Nobel Prize in Physics in 1978 for their discovery.



Figure 1.1: Robert Woodrow Wilson and Arno Penzias in front of their Dicke radiometer.

The interpretation of the cosmic microwave background was highly controversial in the 1960s. Proponents of the steady state theory, a model in which new matter is continuously created as the universe expands, argued that the CMB was the result of scattered starlight from distant galaxies. But new measurements at a range of frequencies showed that the spectrum of the microwave background was a black body spectrum and the steady state theory was unable to reproduce this result. Therefore the consensus was established during the 1970s that the CMB is a remnant of the big bang.

Harrison, Peebles and Yu, and Zel'dovich realized that the early universe would have to have small inhomogeneities. These inhomogeneities would eventually lead to small anisotropies in the cosmic microwave background. The anisotropy of the cosmic background was first detected by the COBE satellite.

Since this discovery it has been tried to map the sky at increasing levels of sensitivity and angular resolution by ground-based and balloon-borne measurements. These maps were joined in 2003 by the first results from NASA's WMAP, the satellite succeeding COBE. This has led to quite a lot information about our universe and it places constraints on a number of cosmological parameters.

# Chapter 2

## Introduction

Just after the big bang the universe was very hot and very dense, [1]. There were no neutral atoms or even nuclei. If a nucleus or atom was produced it would immediately be destroyed by a high energy photon. Matter and radiation were at thermal equilibrium at that time due to these rapid collisions between photons and free electrons, so called Compton scattering. Electrons were tightly coupled to protons via Coulomb scattering.

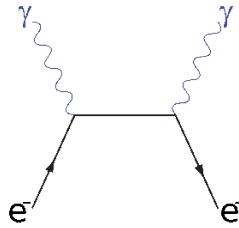


Figure 2.1: Compton Scattering.

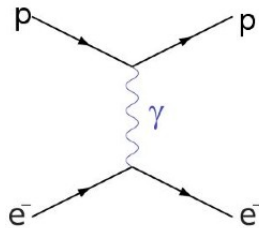


Figure 2.2: Coulomb scattering

As the universe expanded, it cooled down. At some the temperature of the universe dropped below the binding energies of typical nuclei. At that moment light elements started to form. Electrons were bound into neutral atoms, this proces is called recombination. Because of recombination photons could no longer scatter of

of free electrons. Radiation decoupled from matter. This moment is therefore called decoupling.

The surface where this took place, i.e. where the photons last scattered from the free electrons, is called last scattering surface. The photons started freestreaming from that moment on, i.e. they were moving freely through the universe. Thus, the photons which form the cosmic microwave background had their last interaction at the last scattering surface. By measuring the properties of these photons today, e.g. their temperature and their polarization, we can obtain information about the last scattering surface and thus about the early universe.

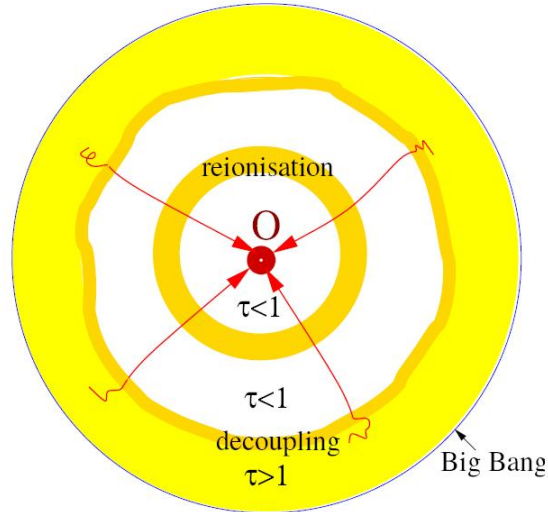


Figure 2.3: A conformal diagram of an expanding universe.  $\tau$  is the optical depth and the red lines pointing inwards are photons. [2]

This process is shown schematically in Figure 2.3. The time direction is inwards. First, the big bang took place, this is the outer circle. Then, there was an epoch of inflation and of thermal equilibrium between matter and radiation. Then, as the temperature of the universe dropped further, decoupling took place at the last scattering surface. In the figure the last scattering surface is depicted by an orange line. From that moment on photons are freestreaming. At a later time reionisation took place and about 17% of the photons rescatter. Even later the photons reach us. We are in the center of the circle.

As said before, before decoupling there are two important types of collisions, namely Coulomb scattering and Compton scattering. Coulomb scattering is an interaction between a proton and an electron (or positron) via a photon. The Feynman diagram of this interaction is shown in Figure 2.2. Compton scattering is the scattering of a photon and a free electron. It is shown in Figure 2.1. First the free electron annihilates the photon and then it emits the photon again. After decoupling electrons were bound into helium atoms and Compton scattering did not take place anymore. Still, photons scattered off by electrons, but now by bound electrons. This scattering process is called Thomson scattering. The cross section of Thomson



scattering is much smaller than the cross section of Compton scattering. Therefore, although there is still some scattering there is no longer a thermal equilibrium. The Thomson scattering is important for the polarization of the photons and we will come back to it in Chapter 7.

This is qualitatively the story of the cosmic microwave background radiation. In the next chapters will take a closer look to the phenomenon and make a more quantitative approach to some of the processes.



# Chapter 3

## Black Body Spectrum

Before decoupling radiation and matter were in thermal equilibrium, [1], [3]. The number density of photons in equilibrium with matter at temperature  $T$  at photon frequency between  $\nu$  and  $\nu + d\nu$  is given by

$$n_T(\nu)d\nu = \frac{8\pi\nu^2 d\nu}{\exp(h\nu/k_B) - 1}, \quad (3.1)$$

where  $h$  is the original Planck's constant and  $k_B$  is the Boltzmann constant. Eq.(3.1) is a so called black body spectrum. After decoupling photons were no longer in thermal equilibrium with electrons and they started free streaming. But the spectrum of the photons has kept the same form.

That the form of the spectrum has stayed the same is most easily seen by assuming that there was one time where radiation went from being in thermal equilibrium with matter to a free expansion. This time is denoted by  $t_L$  where the subscript  $L$  stands for last scattering. A freely moving photon at some later time  $t$  with frequency  $\nu$  would have had at time  $t_L$  a frequency  $\nu a(t)/a(t_L)$ , where  $a(t)$  is the expansion rate at time  $t$ . So the number density of photons with a frequency between  $\nu$  and  $\nu + d\nu$  at time  $t$  would be

$$n(\nu, t)d\nu = \left(\frac{a(t_L)}{a(t)}\right)^3 n_{T(t_L)} \left(\frac{\nu a(t)}{a(t_L)}\right) d\left(\frac{\nu a(t)}{a(t_L)}\right). \quad (3.2)$$

The universe has expanded between the time of last scattering and some later time  $t$  at which we look at the number density of photons. We have to account for this if we want to calculate the number density of photons after expansion. This is why there is a factor  $(a(t_L)/a(t))^3$  in Eq.(3.2). Using Eq.(3.1) in Eq.(3.2) yields for the number density

$$n(\nu, t)d\nu = \frac{8\pi\nu^2 d\nu}{\exp(h\nu/k_B) - 1} = n_{T(t)}(\nu)d\nu, \quad (3.3)$$

where

$$T(t) = T(t_L) \frac{a(t_L)}{a(t)}. \quad (3.4)$$

Thus the form of the spectrum has not changed, namely Eq.(3.3) is still a black body spectrum. But the temperature of the spectrum has changed. The spectrum at a later time  $t$  has a redshifted temperature.

We assumed that radiation decoupled from matter suddenly, but this was not exactly the case. There is a finite time interval during which decoupling took place. In other words, the surface of last scattering has a certain thickness. During this time interval approximately all interactions between photons and matter were elastic scattering processes. In those processes the frequency of a photon does not change. Therefore the conclusion that the spectrum of the photons remains a black body spectrum still holds.

This predicted black body spectrum has been measured with a very high precision, see Figure 3.1. In fact, the spectrum of the cosmic microwave background radiation is the most perfect black body spectrum ever measured. It turns out that this is a very important feature of the cosmic microwave background.

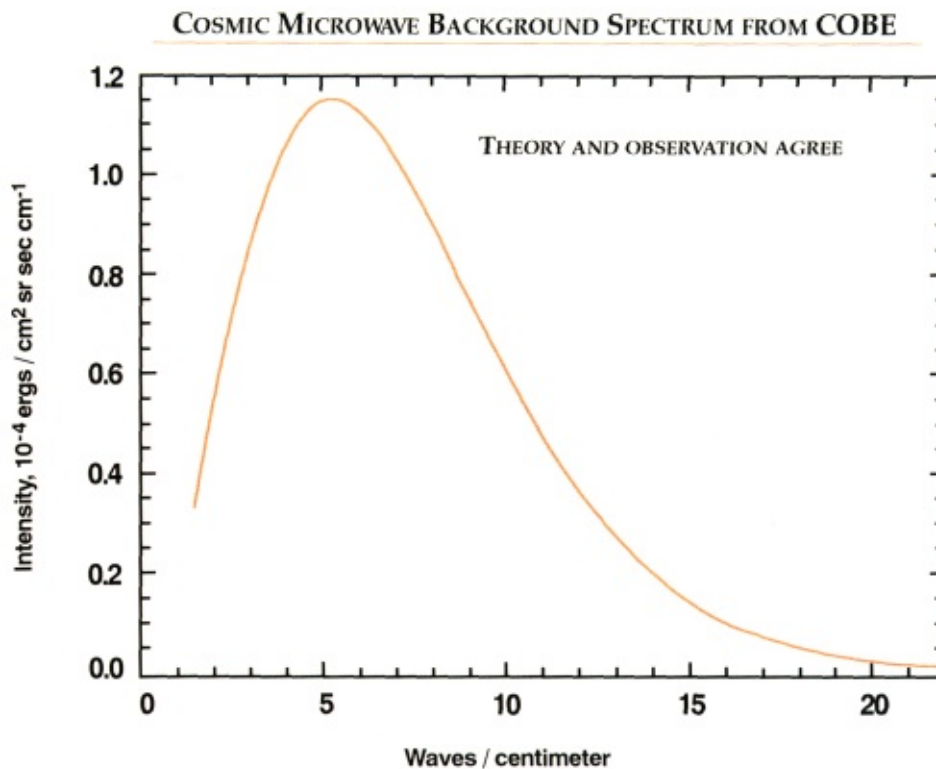


Figure 3.1: The black body spectrum of the cosmic microwave background. The error bars of the measurements are smaller than the thickness of the theoretical curve. What is measured is the intensity of the incoming photons. The intensity is directly related to the number density.

The temperature of the cosmic microwave background is measured to be  $T = 2.725 \pm 0.001 \text{K}$ . From this measurement already information about the early universe can be obtained, namely the redshift of decoupling.

As we saw before decoupling took place at the time when hydrogen atoms started to form. The binding energy of a hydrogen atom is 13.6 eV. From this we can estimate the temperature of the universe at the time of decoupling to be  $T \approx 3000 \text{K}$ . Eq.(3.4) shows that this temperature is rescaled via the ratio of the expansion at last scattering and the expansion rate now. The redshift is related to the expansion rate via

$$a = \frac{1}{1+z}. \tag{3.5}$$

The redshift of decoupling is then found to be  $z_{\text{dec}} = 1089$ .



# Chapter 4

## Measurements of the CMB

Since the discovery of the cosmic microwave background by Penzias and Wilson a lot of measurements have been performed on the CMB. The first measurements on the CMB confirmed that the spectrum would be a black body spectrum. And it was then found that the CMB is isotropic, i.e. the temperature of photons reaching the earth from different directions is the same. Later on, as measurements became more precise, it was found that this is not exactly true. The temperature of the photons is slightly different for different directions. Very important measurements on the CMB have been done by the COBE satellite, the Cosmic Background Explorer, and by the WMAP, the Wilkinson Microwave Anisotropy Probe. The Cosmic Background Explorer is a satellite developed by NASA in the seventies. It was put into sun-synchronous orbit in 1989. From then on it measured the temperature of the photons coming from all directions. It was announced in 1992 that small anisotropies were found in the temperature of the CMB, as measured by COBE. The WMAP was also developed by NASA, to succeed COBE. It was launched in 2001. The WMAP is able to do measurements with a much higher precision than the COBE, [5], [6]. The measurements done by the WMAP further confirm the existence of anisotropies in the temperature of the cosmic microwave background radiation.

### 4.1 Foreground Subtraction

Both the COBE and the WMAP measure the temperature of all incoming photons. These incoming photons will not only be photons from the CMB, but also from a lot of other sources such as our galaxy. To keep this to a minimum the WMAP is put in an orbit behind the earth, such that it will not receive photons coming from the sun (see Figure 4.2).

To obtain information about the CMB a distinction has to be made between photons from the CMB and other photons. Measurements of these other photons have to be subtracted so that we are only left with CMB measurements. This process is called foreground subtraction and it is done in several ways, [4]. Firstly, a lot of measured photons are emitted at known source, such as stars and planets we know. Since the location and the properties of these sources are known, they can be removed from the data. Secondly, it is used that the spectrum of the photons making up

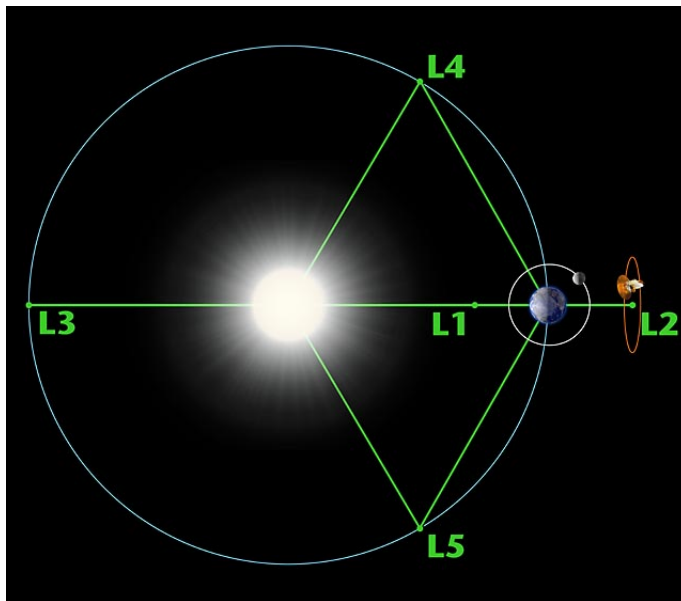


Figure 4.1: The orbit of the Wilkinson Microwave Anisotropy Probe. It is chosen in such a way that the WMAP will not receive photons coming from the sun.

the CMB is a perfect black body spectrum. Photons coming from other sources have a different spectrum and in this way one can distinguish between the different photons. In order to do this observations are made at multiple frequencies.

Although, this sounds like a simple process it is very complicated to actually perform it. Still, very smart scientists have been able to subtract the foreground from the data obtained by the WMAP. The final set of data consists of the measured temperature in all different directions. From this set information can be obtained about anisotropies of the CMB.

## 4.2 Temperature Fluctuations

Thus what is measured is the temperature of photons of the cosmic microwave background coming from different directions. The temperature of the cosmic background is the mean value of all these temperatures.  $T = 2.725 \pm 0.001\text{K}$ .

The temperature differences are then expressed as the difference between the measured temperature and the average temperature. These temperature fluctuations are depicted in Figure 4.2. The fluctuations are very small, of the order  $\mu\text{K}$ .



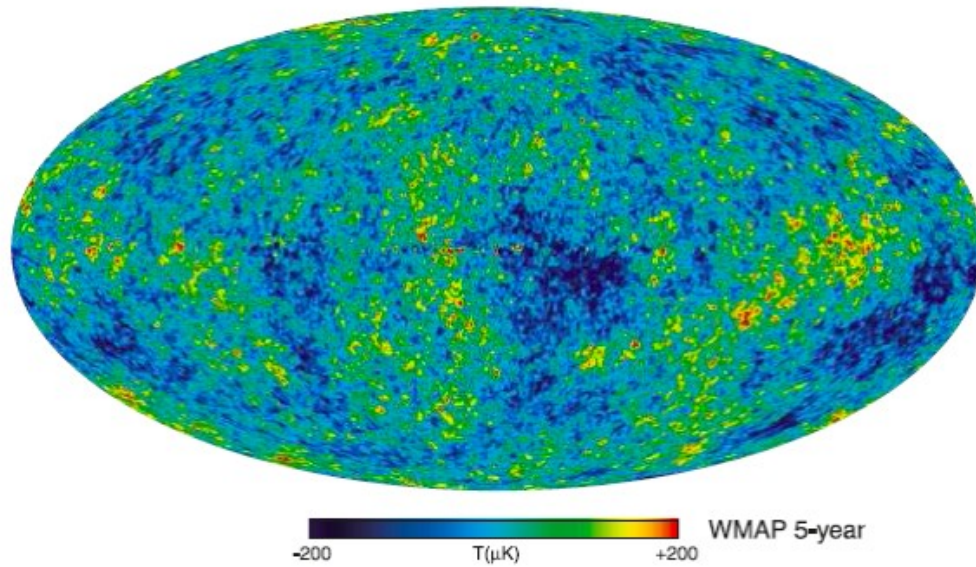


Figure 4.2: The 5 year WMAP image of the cosmic background radiation. The foreground has been subtracted. Of course this is a very pretty picture, but it does not have any scientific purpose. Information about the CMB is obtained directly from the data and not from this picture.

### 4.3 Future Measurements

The satellite to succeed WMAP is already under construction. This is the Planck satellite and it is developed by ESA, [7]. The Planck satellite will be able to observe the anisotropies in the cosmic background with a higher precision and higher angular resolution. Moreover, the Planck satellite will perform measurements on the polarization of the cosmic microwave background.

It is hoped for that the measurements done by the Planck satellite can tell us more about our universe than what measurements so far have already told us. The Planck satellite will be launched in april of 2009.

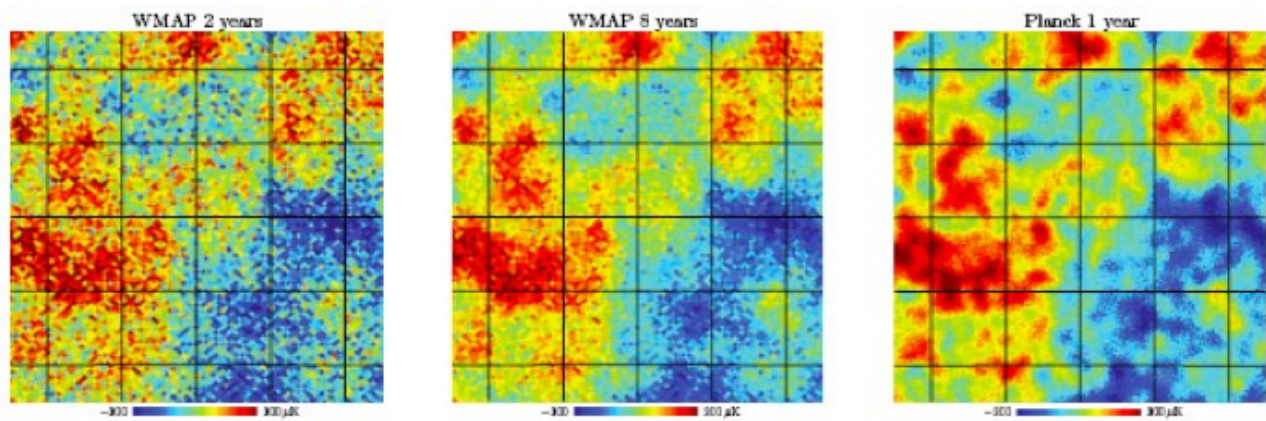


Figure 4.3: Different resolutions of different measurements of the CMB.

# Chapter 5

## Anisotropies in the Cosmic Microwave Background

As already mentioned, it turns out that the cosmic background radiation is not completely isotropic. Instead slightly different temperatures are measured in different directions. These differences are all with respect to the mean value, which can be considered as the monopole term.

There are two kinds of anisotropies. Anisotropies which have their origin in the very early universe, called primary anisotropies, and anisotropies which were caused later on. An example of this second kind of anisotropies is the Doppler shift in the temperature due to the motion of the earth with respect to the CMB. This is the dipole anisotropy and will be discussed in more detail, [3], [4].

### 5.1 The Dipole Anisotropy

To analyse the dipole anisotropy it is useful to look at the density of photons in phase space  $N_\gamma(\mathbf{p})$

$$N_\gamma(\mathbf{p}) = \frac{1}{\hbar} \frac{1}{\exp(|\mathbf{p}|c/kT) - 1}. \quad (5.1)$$

This would be the density of photons measured by an observer at rest with respect to the radiation background. The phase space volume is Lorentz invariant and the number of photons is also Lorentz invariant. Thus, the density of photons in phase space is a scalar in the sense that a Lorentz transformation that transforms  $\mathbf{p}$  to  $\mathbf{p}'$  also transforms  $N_\gamma$  to  $N'_\gamma$ , where

$$N'_\gamma(\mathbf{p}') = N_\gamma(\mathbf{p}). \quad (5.2)$$

If the earth is moving in the three-direction with velocity  $\beta$  with respect to the cosmic background and we take  $\mathbf{p}$  to be the momentum of a photon in the frame at rest in the cosmic background and  $\mathbf{p}'$  to be the photon momentum in the frame of

the earth, then

$$\begin{pmatrix} p_1 \\ p_2 \\ p_3 \\ |\mathbf{p}| \end{pmatrix} = \begin{pmatrix} 1 & 0 & 0 & 0 \\ 0 & 1 & 0 & 0 \\ 0 & 0 & \gamma & \beta\gamma \\ 0 & 0 & \beta\gamma & \gamma \end{pmatrix} \begin{pmatrix} p'_1 \\ p'_2 \\ p'_3 \\ |\mathbf{p}'| \end{pmatrix},$$

where  $\gamma \equiv (1 - \beta^2)^{-1/2}$ . In particular one finds for the momentum

$$|\mathbf{p}| = \gamma(1 + \beta \cos \theta') |\mathbf{p}'|, \quad (5.3)$$

where  $\theta'$  is the angle between  $\mathbf{p}$  and the three-axis. Thus for the density of photons in a moving frame one finds

$$N'_\gamma(\mathbf{p}') = \frac{1}{\hbar} \frac{1}{\exp(|\mathbf{p}'|c/kT') - 1}. \quad (5.4)$$

The temperature is here a function of the angle between the motion of the photon and the motion of the earth. It is given by

$$T'(\theta) = \frac{T}{\gamma(1 + \beta \cos \theta)}. \quad (5.5)$$

Thus we expect a direction in which the temperature of the photons is maximal and we expect the photons coming from the opposite direction to have a minimal temperature. From this the motion of the earth with respect to the cosmic background can be deduced.

The WMAP satellite experiment has found this maximum temperature increase of  $3.346 \pm 0.017 \text{mK}$  to be in the direction  $\ell = 263^\circ.85 \pm 0^\circ.1$ ,  $b = 48^\circ.25 \pm 0^\circ.04$ . These results indicate a motion of the solar system with a velocity  $(0.00335)c/(2.725) = 370 \text{km/s}$ . The earth has a velocity relative to the center of the galaxy of about  $215 \text{km/s}$ , more or less in the opposite direction. Taking this into account we can find the net velocity of the local group of galaxies relative to the cosmic background. This yields  $627 \pm 22 \text{km/s}$  in a direction ( $\ell = 276^\circ \pm 3^\circ$ ,  $b = 30^\circ \pm 3^\circ$ ).

Eq.(5.5) can be expanded in powers of  $\beta$ . Expressed in terms of Legendre polynomials it then becomes

$$\Delta T \equiv T' - T \quad (5.6)$$

$$= T \left[ -\frac{\beta^2}{6} - \beta P_1(\cos \theta) + \frac{2\beta^2}{3} P_2(\cos \theta) + \dots \right]. \quad (5.7)$$

Since  $\beta$ , the velocity of the earth with respect to the cosmic background, is a small number, the shift in the temperature consists mainly of a dipole term,  $P_1$ . But there is also a small quadropole term. This quadropole term is not much smaller than the quadropole term of the primary anisotropies.

The dipole is a frame-dependent quantity, since it is caused by the motion of the earth. From the dipole it is possible to determine the absolute rest frame. This would be the frame in which the cosmic microwave background dipole term is zero. Normally, our velocity with respect to the Local Group, as well as the velocity of the earth around the sun is removed for purposes of CMB anisotropy study.

## 5.2 Primary Fluctuations in the CMB

Small anisotropies have been found in the cosmic microwave background. These anisotropies result from small perturbations in the energy density of the very early universe. Hence the detection of these anisotropies has provided evidence for the existence of the density perturbations in the early universe. And by studying the anisotropies in the CMB information about these perturbations can be found. In order to do this it is convenient to expand the temperature difference  $\Delta T(\hat{n})$  between the temperature measured in the direction of the unit vector  $\hat{n}$  and the mean value of the temperature  $T_0$  in terms of spherical harmonics  $Y_m^\ell(\hat{n})$

$$\Delta T(\hat{n}) \equiv T(\hat{n}) - T_0 = \sum_{\ell m} a_{\ell m} Y_\ell^m(\hat{n}), \quad T_0 \equiv \frac{1}{4\pi} \int d^2\hat{n} T(\hat{n}). \quad (5.8)$$

The sum over  $\ell$  runs over all positive integers and  $m$  runs from  $-\ell$  to  $\ell$ . The choice for an expansion in terms of spherical harmonics is logical since we expect the last scattering surface to be spherical. The temperature difference  $\Delta T(\hat{n})$  is real and therefore there is the reality condition

$$a_{\ell m}^* = a_{\ell -m}. \quad (5.9)$$

In cosmology the quantities of interest are averages. These averages are either averages over all positions in space or ensemble averages. The ergodic theorem states that under reasonable assumptions these two types of averages are the same. The average of a quantity  $A$  will be denoted by  $\langle A \rangle$ , where this can now either mean an average over position or an ensemble average. Furthermore it is assumed that the universe is rotationally invariant on the average, i.e.  $\langle T(\hat{n}_1)T(\hat{n}_2)T(\hat{n}_3)\dots \rangle$  is an invariant function of  $\hat{n}_1$  etc.

Looking at the temperature fluctuations, the simplest non-trivial quantity to look at is the average of two  $\Delta T$ s. This quantity has to be rotational invariant and therefore we have the following restriction for the product of two  $a_{\ell m}$ s

$$\langle a_{\ell m} a_{\ell' m'}^* \rangle = \delta_{\ell, \ell'} \delta_{m, -m'} C_\ell. \quad (5.10)$$

The average of the product of two temperature differences now reads

$$\langle T(\hat{n})T(\hat{n}') \rangle = \sum_{\ell m} C_\ell Y_\ell^m(\hat{n}) Y_\ell^{-m}(\hat{n}') \quad (5.11)$$

$$= \sum_{\ell} C_\ell \left( \frac{2\ell + 1}{4\pi} \right) P_\ell(\hat{n} \cdot \hat{n}'), \quad (5.12)$$

where the sum over  $m$  is performed in the second line and yields a Legendre polynomial  $P_\ell$ . This relation can be inverted to obtain an expression for the multipole coefficients  $C_\ell$

$$C_\ell = \frac{1}{4\pi} \int d^2\hat{n} d^2\hat{n}' P_\ell(\hat{n} \cdot \hat{n}') \langle \Delta T(\hat{n}) \Delta T(\hat{n}') \rangle. \quad (5.13)$$

The multipole coefficients  $C_\ell$  are real and positive. The  $\ell$  is related to the angle  $\theta$  between different directions  $\hat{n}$  by  $\ell \sim 1/\theta$ . Thus large  $\ell$ s correspond to small angles  $\theta$  and vice versa.

The average in Eq.(5.13) can be computed in two manners. One way would be to average over all positions in the universe, but this is impossible for observers on earth. The other way would be to prepare a large number of universes and measure  $\Delta T(\hat{n})$  in each of these universes and average over these measurements. But this is also impossible. The best we can do is compute

$$C_\ell^{\text{obs}} \equiv \frac{1}{4\pi} \int d^2\hat{n} d^2\hat{n}' P_\ell(\hat{n} \cdot \hat{n}') \Delta T(\hat{n}) \Delta T(\hat{n}'). \quad (5.14)$$

Then the question is how good is this approximation for  $C_\ell$ . Therefore, one would like to know the fractional difference between these two quantities. This fractional difference is called the cosmic variance and is given by

$$\left\langle \left( \frac{C_\ell - C_\ell^{\text{obs}}}{C_\ell} \right) \left( \frac{C_{\ell'} - C_{\ell'}^{\text{obs}}}{C_{\ell'}} \right) \right\rangle = \delta_{\ell,\ell'} \frac{2}{2\ell + 1}. \quad (5.15)$$

This expression goes to zero for large  $\ell$ . Thus for large  $\ell$  (small angles),  $C_\ell^{\text{obs}}$  hardly differs from  $C_\ell$ . For small  $\ell$  the difference is larger, so their the uncertainty in  $C_\ell$  (see Figure 5.1).

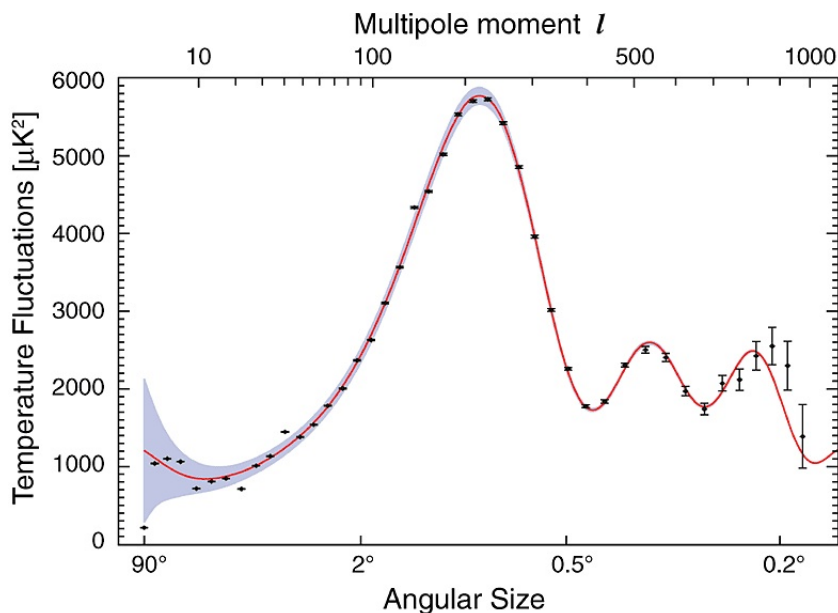


Figure 5.1: The power spectrum of the cosmic microwave background. The blue region denotes the cosmic variance. It is large for small  $\ell$  and it disappears at large  $\ell$ .

Thus for  $\ell < 5$  the cosmic variance is too big for  $C_\ell^{\text{obs}}$  to be of any cosmological interest. And for  $\ell > 2000$  the uncertainty in  $C_\ell^{\text{obs}}$  becomes too large due to foreground effects to be of any interest. To obtain information about the universe we are restricted to the region between 5 and 2000, still a rather large region.

The temperature fluctuations in the CMB at higher multipoles ( $\ell \geq 2$ ) are interpreted as being mostly the result of perturbations in the density of the very early universe and then especially at the surface of last scattering. Though all higher multipoles result from perturbations in the density, they do not all have exactly the same origin. Different regions in  $\ell$  have different physical origins. There are roughly 4 main regions as shown in Figure 5.2, namely the ISW rise, the Sachs-Wolfe plateau, the acoustic peaks and the damping tail. The Sachs-Wolfe plateau will be discussed in some detail. Namely, for this region it is possible to do some analytical calculations. For the other regions the origin of the anisotropies will be discussed, [3], [4].

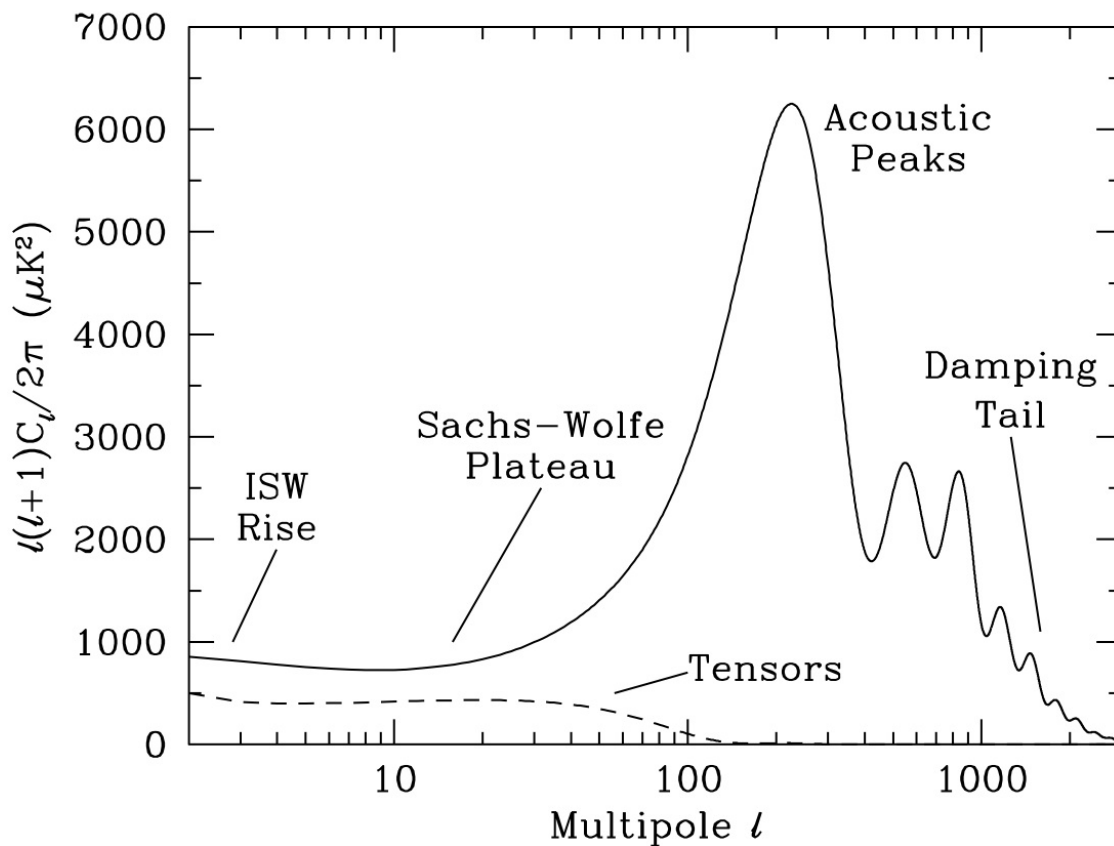


Figure 5.2: The theoretical CMB power spectrum. Used is a standard  $\Lambda$ CDM model from *CMBFAST*. The different regions are labeled: the ISW rise; Sachs-Wolfe plateau; acoustic and damping tail, [4].

### 5.2.1 The ISW rise, $\ell \lesssim 10$ , and Sachs-Wolfe plateau, $10 \lesssim \ell \lesssim 100$

The large angle effect (small  $\ell$ ) result from perturbations in the gravitational potential at the time of last scattering. This is called the Sachs-Wolfe effect, because Sachs and Wolfe were the first to calculate this effect in 1967. The region where this effect is important is for  $10 \geq \ell \geq 100$ . Small potential wells in the early universe plasma would attract matter and the wells would get even deeper. Photons emitted from such a potential well have a shifted frequency and thus a temperature shifted from the average temperature by an amount

$$\left(\frac{\Delta T(\hat{n})}{T_0}\right) = \delta\phi(\hat{n}r_L), \quad (5.16)$$

where  $r_L$  is the radial coordinate of the surface of last scattering, given by

$$r_L = \frac{1}{\Omega_K^{1/2} H_0 a(t_0)} \sinh \left[ \Omega_K^{1/2} \int_{1/(1+z_L)}^1 \frac{dx}{\sqrt{\Omega_\Lambda x^4 + \Omega_K x^2 + \Omega_M x + \Omega_R}} \right], \quad (5.17)$$

where  $\Omega_K = 1 - \Omega_\Lambda - \Omega_M - \Omega_R$ ;  $z_L$  is the redshift of last scattering,  $z_L \approx 1089$ ; and  $t_0$  is today. The perturbation to the gravitational has also an effect on the expansion rate, it shifts the expansion rate by an amount of  $\delta\phi(\mathbf{x})$ . And since the temperature in a matter-dominated universe scales as  $a^{-1}$  this shifts the redshift at which the universe reaches the surface of last scattering in a certain direction  $\hat{n}$  by a fractional amount

$$\left(\frac{\delta z}{1+z}\right)_{T=3000\text{K}} = - \left(\frac{\delta a(t)}{a(t)}\right)_{T=3000\text{K}} = \left(\frac{\dot{a}}{a}\right)_{T=3000\text{K}} \quad (5.18)$$

$$\delta\phi(r_L \hat{n}) t_L = \frac{2}{3} \delta\phi(r_L \hat{n}). \quad (5.19)$$

This effect will shift the observed temperature in the direction  $\hat{n}$  by a fractional amount

$$\left(\frac{\Delta T(\hat{n})}{T_0}\right) = -\frac{2}{3} \delta\phi(\hat{n}r_L). \quad (5.20)$$

Thus, the Sachs-Wolfe effect consists actually of two effects, namely a shift in the temperature due to a perturbation in the gravitational potential and a shift in the temperature due to the fact that the expansion rate is effected by a perturbation in the gravitational potential. The sum of these two effects gives the total Sachs-Wolfe effect. This is the sum of Eq.(5.16) and Eq.(5.20) and yields

$$\left(\frac{\Delta T(\hat{n})}{T_0}\right)_{\text{SW}} = \frac{1}{3} \delta\phi(\hat{n}, r_L). \quad (5.21)$$

To further study this effect a closer look to the gravitational potential is needed. It is convenient to write  $\delta\phi(\mathbf{x})$  as a Fourier transform

$$\delta\phi(\mathbf{x}) = \int d^3q e^{i\mathbf{q}\cdot\mathbf{x}} \delta\phi_{\mathbf{q}}. \quad (5.22)$$



The exponential can be written in terms of Legendre polynomials in the following way

$$e^{i\mathbf{q}\cdot\mathbf{x}} = \sum_{\ell} (2\ell + 1) i^{\ell} P_{\ell}(\hat{q} \cdot \hat{n}) j_{\ell}(qr), \quad (5.23)$$

where  $j_{\ell}$  is the spherical Bessel function. The total Sachs-Wolfe effect, Eq.(5.21), then becomes

$$\left( \frac{\Delta T(\hat{n})}{T_0} \right)_{\text{sw}} = \frac{1}{3} \sum_{\ell=0}^{\infty} (2\ell + 1) i^{\ell} \int d^3q \delta\phi_{\mathbf{q}} j_{\ell}(qr_L) P_{\ell}(\hat{q} \cdot \hat{n}) \quad (5.24)$$

Again, we want to calculate the average of a product of two fractional temperature shifts in two different directions. Although the gravitational potential depends on the position, the probability distribution of  $\delta\phi(\mathbf{x})$  is invariant under spatial rotations and translations. This implies that

$$\langle \delta\phi_{\mathbf{q}} \delta\phi_{\mathbf{q}'} \rangle = \mathcal{P}_{\phi}(q) \delta^3(\mathbf{q} + \mathbf{q}'), \quad (5.25)$$

where  $\mathcal{P}_{\phi}(q)$  depends only on the magnitude of the momentum. And because the gravitational potential is real it follows that  $\mathcal{P}_{\phi}(q)$  is real and positive.

Now using the above properties together with Eq.(5.24) and the orthogonality of the Legendre polynomials results in

$$\langle \Delta T(\hat{n}) \Delta T(\hat{n}') \rangle_{\text{sw}} = \frac{4\pi T_0^2}{9} \sum_{\ell} (2\ell + 1) P_{\ell}(\hat{n} \cdot \hat{n}') \int_0^{\infty} q^2 dq \mathcal{P}_{\phi}(q) j_{\ell}^2(qr_L). \quad (5.26)$$

This result can, as before, be rewritten into an expression for the multipole coefficients

$$C_{\ell, \text{sw}} = \frac{16\pi^2 T_0^2}{9} \int_0^{\infty} q^2 dq \mathcal{P}_{\phi}(q) j_{\ell}^2(qr_L). \quad (5.27)$$

An educated guess for the form of  $\mathcal{P}_{\phi}(q)$ , when the gravitational potential is produced by cold dark matter, is a rather simple form, such as a power of  $q$ . This is often written as

$$\mathcal{P}_{\phi}(q) = N_{\phi}^2 q^{n-4}, \quad (5.28)$$

where  $N_{\phi}^2$  is a positive constant and  $n$  is called the scalar spectral index. To compute  $\langle \Delta T(\hat{n}) \Delta T(\hat{n}') \rangle_{\text{sw}}$  we can use the standard formula for the spherical Bessel function

$$\int_0^{\infty} j_{\ell}^2(s) s^{n-2} ds = \frac{2^{n-4} \pi \Gamma(3-n) \Gamma(\ell + \frac{n-1}{2})}{\Gamma^2(\frac{4-n}{2} \Gamma(\ell + 2 - \frac{n-1}{2}))}. \quad (5.29)$$

For  $\ell < 100$  we then find for the multipole coefficients

$$C_{\ell \text{sw}} \rightarrow \frac{16\pi^3 2^{n-4} \Gamma(3-n) r_L^{1-n} N_{\phi}^2 T_0^2}{9\Gamma^2(\frac{4-n}{2})} \frac{\Gamma(\ell + \frac{n-1}{2})}{\Gamma(\ell + 2 - \frac{n-1}{2})}. \quad (5.30)$$

For  $n = 1$  this reduces to

$$C_{l,\text{SW}} \rightarrow \frac{8\pi^2 N_\phi^2 T_0^2}{9l(l+1)}. \quad (5.31)$$

The value for  $n$  can be found by studying the cosmic microwave background and it turns out that it is close to 1, but it is not exactly 1. Eq.(5.31) shows that in this region for  $l$ ,  $l(l+1)C_\ell$  is constant. This can also be seen in Figure 5.2 where  $l(l+1)C_\ell$  is plotted instead of  $l$  for exactly this reason. And this also explains the name plateau.

This calculation was only for small perturbations in the gravitational potential during time of last scattering. But there can also be small perturbations on the way between the last scattering and us which the photons have to pass. These perturbations will also effect the frequency of the photon, but only if the perturbations are time-dependent. If the perturbation was time-independent, the blueshift caused by the photon falling into the potential well would be exactly cancelled by the redshift caused when the photon climbs out of the well.

To calculate this effect one has to perform a line integral along the path of the photon. This effect is therefore called the integrated Sachs-Wolfe effect. It is the most important effect for the multipole coefficients with  $l \lesssim 10$ . For larger  $l$  the Sachs-Wolfe effect becomes larger and dominates.

### 5.2.2 The acoustic peaks, $100 \lesssim l \lesssim 1000$

Before decoupling, there was a plasma consisting of baryons and photons in which there was a thermal equilibrium between radiation and matter. In this plasma, perturbations in the gravitational were steadily evolving. They drove oscillations in the plasma, thus the density underwent oscillations. This gave time variations in the temperature.

At decoupling, the phases of the sound waves were frozen-in, and became projected on the sky as a harmonic series of peaks, see Figure 5.2. The main peak is the mode that went through 1/4 of a period, reaching maximal compression. The even peaks correspond to maximal under-densities and the odd peaks to maximal over-densities. The under-density peaks are generally have a smaller amplitude because the photons which come from an under-density have to fight against the baryon inertia.

These peaks were first detected in 1994, although they were already predicted in the 1970s.

### 5.2.3 The damping tail, $l \gtrsim 1000$

As said before, the recombination process is not instantaneous. This means that the last scattering surface had a certain thickness. This leads to a damping of the anisotropies corresponding to scales smaller than that subtended by this thickness. Small angles correspond to high  $l$ , thus the multipole coefficients at the highest  $l$  get damped. This is called the damping tail, see Figure 5.2.

# Chapter 6

## Constraints on Theories and Cosmological Parameters

The anisotropies in the cosmic microwave background can be measured with a rather high precision and it is still improving. Thus, there is a rather good picture of what the power spectrum of the CMB, [8].

As pointed out in the last chapter, these anisotropies mostly result from our early universe and are then mainly caused by perturbations on the gravitational potential. And the gravitational potential is in turn produced by cold dark matter and has some initial conditions.

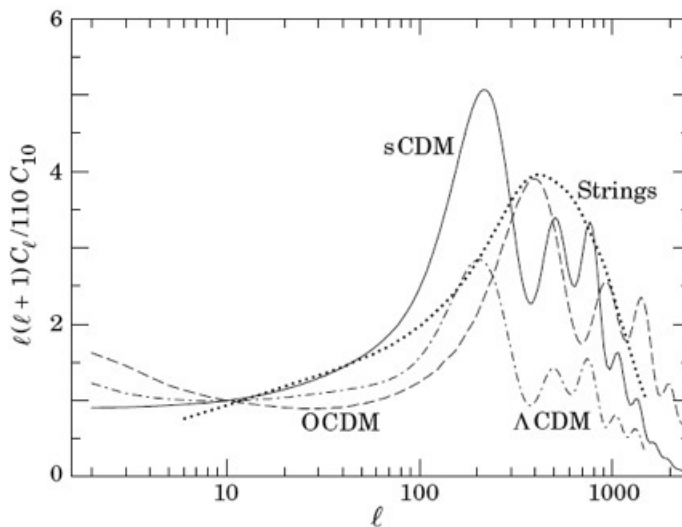


Figure 6.1: Different theories predict different power spectra of the cosmic microwave background. **sCDM** is the standard cold dark matter model with  $h = 0.5$  and  $\Omega_B = 0.05$ .  **$\Lambda$ CDM** is a cold dark matter model with  $\Omega_{\text{tot}} = \Omega_\Lambda + \Omega_0 = 1$ , with  $\Omega_\Lambda = 0.3$  and  $h = 0.8$ . **OCDM** is an open model with  $\Omega_0 = 0.3$  and  $h = 0.75$ . **Strings** is a model where cosmic strings are the main source of large scale structure formation, [9]

If there is a theory describing the early universe and in particular, describing the gravitational potential, it should at least be able to reproduce the CMB power spectrum. Otherwise the theory does not fit with the experiments. Thus, the cosmic microwave background gives constraints on the possible theories describing our universe.

In Figure 6.1 different predicted power spectra are plotted. It can be seen that the String theory does not predict the acoustic peaks. Therefore it is ruled out as a possible theory describing the early universe. The other theories, the different cold dark matter models, do show acoustic peaks. But at different values for  $\ell$  and with different heights.

All theoretical models also contain parameters, such as the Hubble parameter and the scalar spectral index. The cosmic microwave background does not only constrain possible theories but also the cosmological parameters.

In Figure 6.2 it is shown that different values for a parameter result in different power spectra.

There are some combinations of parameters that fit the CMB spectrum almost equivalently. For example, any combination of  $\Omega_M$  and  $\Omega_\Lambda$  that gives the same angular diameter distance to the last scattering surface will give almost identical multipole coefficients.

From the WMAP-5 year data a list of the cosmological parameters is made which fit the best. A  $\Lambda$ CDM model is used for this. The values are listed in Table 6.1.

Table 6.1: Cosmological parameters

Parameter	Symbol	Value
Age of the universe	$t_0$	$13.69 \pm 0.13$ Gyr
Hubble constant	$H_0$	$71.9^{+2.6}_{-2.7}$ km/s/Mpc
Baryon density	$\Omega_b h^2$	$0.02273 \pm 0.00062$
Dark matter density	$\Omega_c h^2$	$0.1099 \pm 0.0062$
Dark energy density	$\Omega_\Lambda$	$0.742 \pm 0.030$
Curvature fluctuation amplitude	$\Delta_{\mathcal{R}}^2$	$(2.41 \pm 0.11) \times 10^{-9}$
Scalar spectral index	$n_s$	$0.963^{+0.014}_{-0.015}$
Redshift of decoupling	$z^*$	$1090.51 \pm 0.95$

The fit made in Figure 5.1 is also made using a  $\Lambda$ CDM model where the values of Table 6.1 are used for the cosmological parameters. An analytical calculation for the power spectrum is not possible. To make these fits computer programs, such as CMBFAST and CAMB, are used.

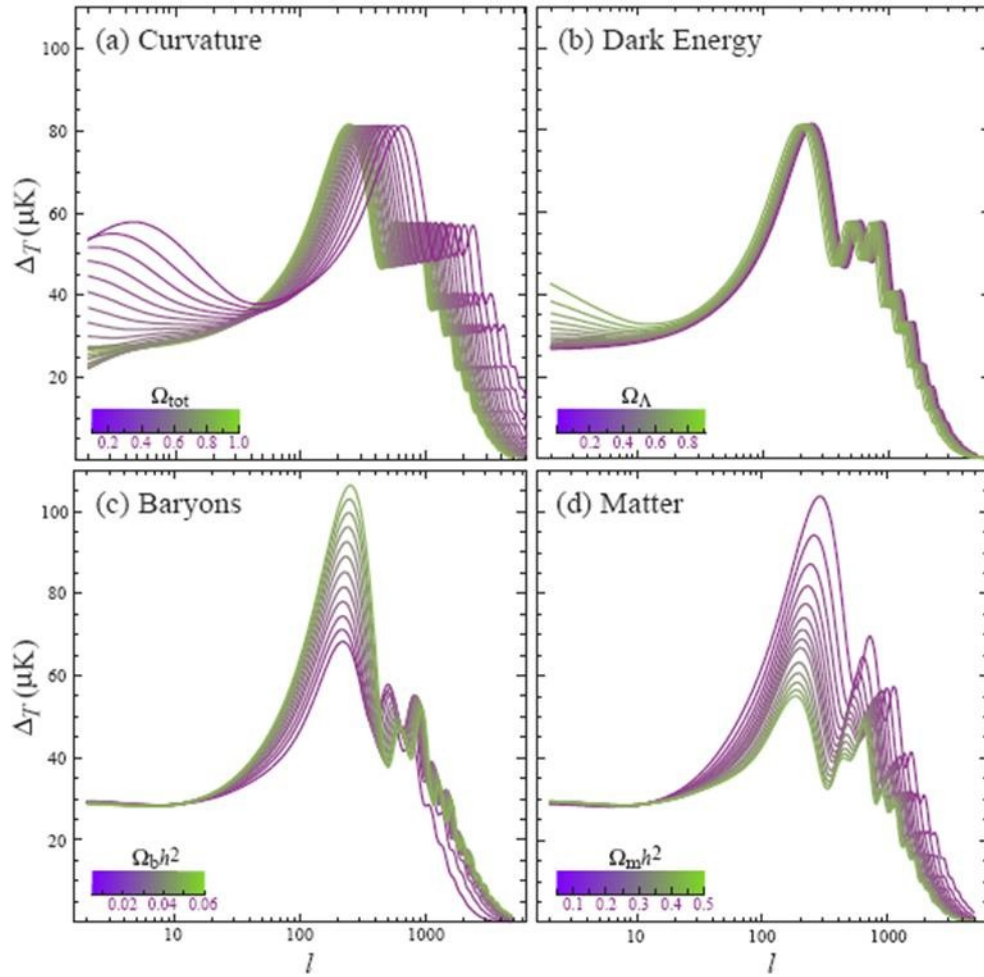


Figure 6.2: Using different values for cosmological parameters results in different power spectra. In (a) the curvature is varied via  $\Omega_{\text{tot}}$ , in (b) the dark energy density, in (c) the baryon density and in (d) matter density.



# Chapter 7

## Polarization

Until so far, we have only discussed anisotropies in the temperature spectrum of the cosmic background. It turns out, that these are not the only anisotropies in the CMB.

Apart from the temperature, the polarization of the incoming photons can also be measured, and it turns out that the polarization of the photons is not the same for all directions. This is expected because of scattering of the radiation by free electrons at the time around recombination or during reionization. Information about the polarization is important because the beginning of reionization can be learned from it and it can be used to disentangle the effect of reionization from the primordial fluctuations. And in the future they might even reveal the effects of gravitational waves produced during inflation. WMAP has already done some measurements on the polarization of the CMB (see Figure 7.1) and it is expected that much more information on the polarization of the CMB will be obtained by the Planck satellite.

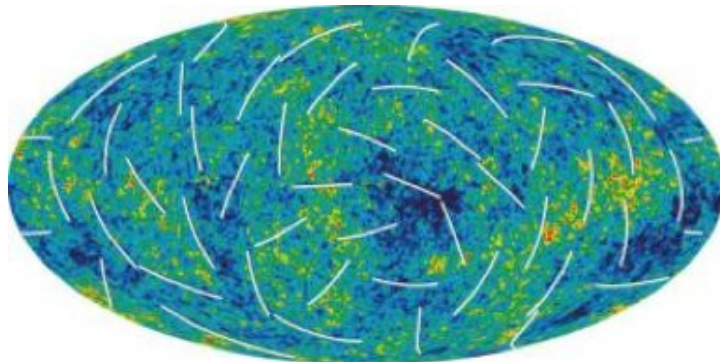


Figure 7.1: Polarization of the cosmic microwave background as measured by the WMAP satellite

The polarization anisotropies will not be discussed in as much detail as the temperature anisotropies were discussed. The main idea is the same: the polarization fluctuations can be expanded in spherical harmonics and this can be inverted to obtain an expression for the coefficients. And then a power spectrum can be created,

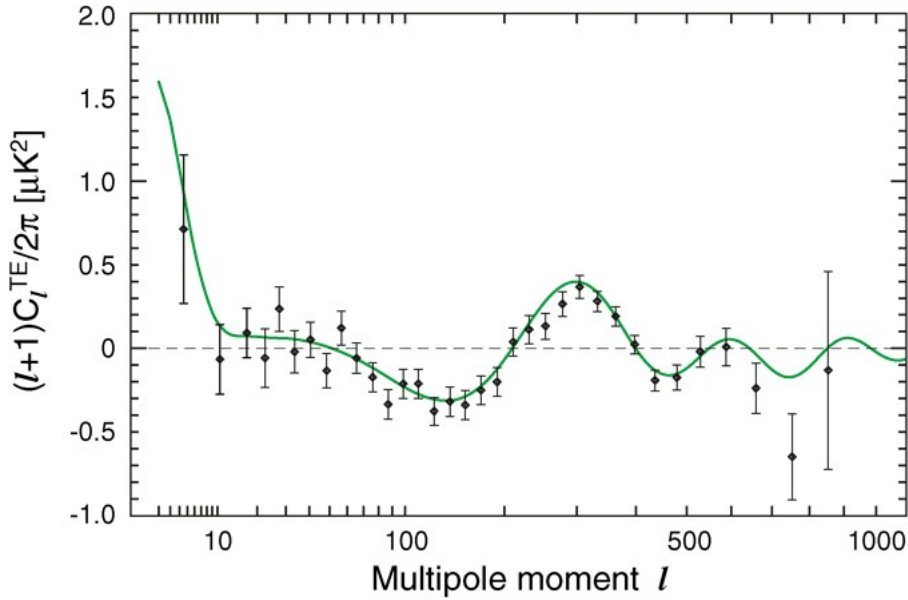


Figure 7.2: The power spectrum for the polarization of the cosmic microwave background as found by WMAP.

see Figure 7.2.

What will be discussed is how Thomson scattering produces polarization, [10]. Suppose we have a free electron and radiation coming in from four directions, see Figure 7.3, from the  $\pm\hat{x}$  and  $\pm\hat{y}$  directions. If the intensities of these radiations is the same, then the polarizations of the scattered radiation will cancel, i.e. the scattered radiation will be unpolarized. But if the intensities are slightly different, then the different polarizations will not cancel and the scattered radiation will be polarized.

Small intensity fluctuations are present at the surface of last scattering, this is what the power spectrum of the temperature fluctuations shows. Therefore, it is not unexpected that the cosmic background is polarized.

The angular dependence of Thomson scattering is

$$\frac{d\sigma}{d\Omega} = \frac{3\sigma_T}{8\pi} |\hat{\epsilon}' \cdot \hat{\epsilon}|^2, \quad (7.1)$$

where  $d\Omega = \sin\theta d\theta d\phi$ ,  $\sigma_T$  is the Thomson cross section, and  $\hat{\epsilon}'$  and  $\hat{\epsilon}$  are the polarization of the incident and scattered radiation, respectively. From this it can be shown that radiation scattered from an electron cloud must be polarized.



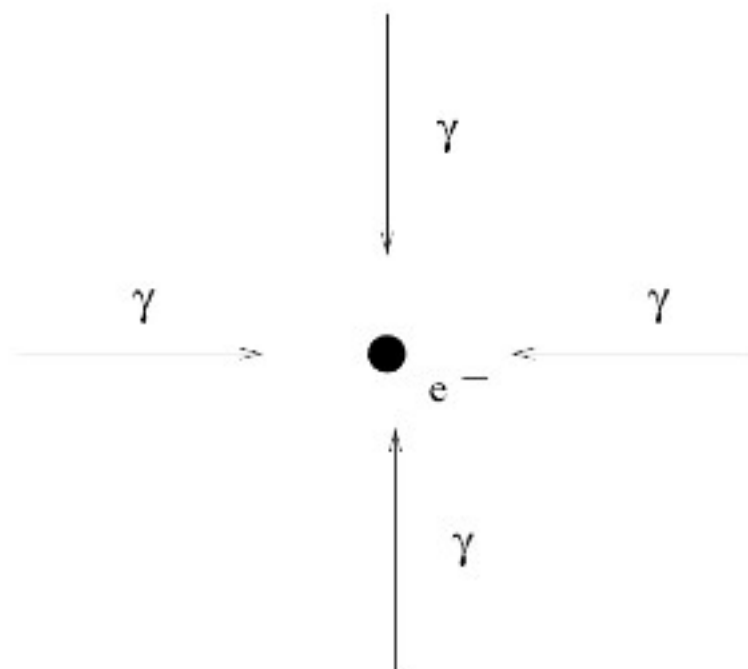


Figure 7.3: Radiation incident on an electron.



# Bibliography

- [1] S. Dodelson, *Modern Cosmology*  
Academic Press, Massachusetts (2003)
- [2] T. Prokopec, *Lecture notes on Cosmology*
- [3] S. Weinberg, *Cosmology*  
Oxford University Press, 2008
- [4] D. Scott and G. F. Smoot, *Cosmic Microwave Background*, Physics Letters **B667**, 1 (2008)  
(URL: <http://pdg.lbl.gov/>)
- [5] G. Hinshaw *et al*, *First Year Wilkinson Microwave Anisotropy Probe (WMAP) Observations: The Angular Power Spectrum* (2003)  
arXiv:astro-ph/0302217v1
- [6] E. Komatsu *et al.*, *Five-Year Wilkinson Microwave Anisotropy Probe (WMAP) Observations: Cosmological Interpretation* (2008)  
arXiv:astro-ph/0803.054/v2
- [7] Planck Experiment: <http://www.rssd.esa.int/index.php?project=PLANCK>
- [8] A. de Oliveira-Costa *et al.*, *The significance of the largest scale CMB fluctuations in WMAP* (2003)  
arXiv.org:astro-ph/0307282v3
- [9] L. Montranet *et al.*, Physical Review **D50**, 1173 (1994)  
(URL: <http://pdg.lbl.gov/>)
- [10] P. Cabella and M. Kamionkowski, *Theory of cosmic microwave background polarization*, Lectures given at the 2003 Villa Mondragone School of Gravitation and Cosmology: "The Polarization of the Cosmic Microwave Background," Rome, Italy, September 6-11, 2003.  
arXiv:astro-ph/0403392v2